ACS APPLIED POLYMER MATERIALS

pubs.acs.org/acsapm

Article

Mechanically Strong Superabsorbent Terpolymer Hydrogels Based on AMPS via Hydrogen-Bonding Interactions

Busra Sekizkardes, Esra Su,* and Oguz Okay*

Cite This: *ACS Appl. Polym. Mater.* 2023, 5, 2043−2050

Read Online

ACCESS | Metrics & More | Article Recommendations | Supporting Information

ABSTRACT: Polymers based on 2-acrylamido-2-methyl-1-propanesulfonic acid (AMPS) attract significant attention due to their large water absorption capacity when swollen in water. Poly(AMPS) (PAMPS) hydrogels are usually synthesized via free-radical cross-linking copolymerization of AMPS and a chemical cross-linker in aqueous solutions. Owing to the covalently cross-linked network structure of PAMPS hydrogels preventing dissipation of the crack energy, they exhibit poor mechanical properties. Herein, we demonstrate that the terpolymerization of AMPS, methacrylic acid (MAAc), and *N*,*N*-dimethylacrylamide (DMAA) in an aqueous solution under UV light without a chemical cross-linker produces mechanically strong hydrogen-bonded hydrogels that are durable in water. The terpolymer hydrogels formed at a MAAc/DMAA molar ratio of 4:1 exhibit a high Young's modulus (26 ± 2 MPa) and toughness (31 ± 5 MJ·m^{-3}) and are able to absorb 2035 ± 255 times their mass in water without dissolving. The water content at the gel preparation, denoted by *w*, significantly affects the microstructure of terpolymer hydrogels. Decreasing the water content *w* at gelation increases the length of the primary chains forming the three-dimensional (3D) network and hence the number of interchain H-bonds due to the proximity effect. An optically transparent-to-opaque transition accompanied with a strong-to-weak transition in the mechanical properties was detected with increasing *w* due to the transformation of the uniform network into a colloidal network composed of phase-separated and highly hydrogen-bonded AMPS-poor aggregates interconnected by AMPS-rich terpolymer chains.

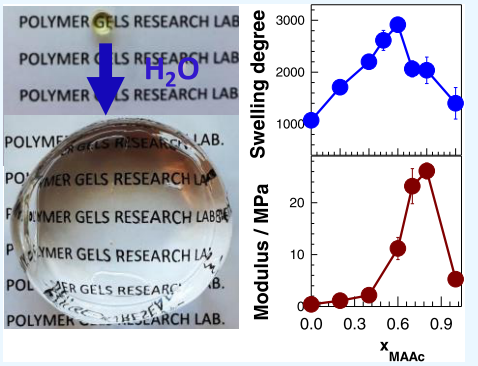

KEYWORDS: *superabsorbent hydrogels, physical hydrogels, hydrogen bonding, mechanical properties, viscoelasticity*

1. INTRODUCTION

Polymers based on 2-acrylamido-2-methyl-1-propanesulfonic acid (AMPS) attract significant attention due to their large water absorption capacity when swollen in water.[1−5] Poly(AMPS) (PAMPS) hydrogels find applications in water purification, bioengineering, agriculture, hygienic products, food engineering, and electrosensitive soft materials.[6−10] PAMPS hydrogels are usually synthesized via free-radical polymerization of AMPS with a chemical cross-linker, and therefore, they exhibit poor mechanical properties because of their covalently cross-linked network structure with low energy dissipation. To improve the mechanical properties, one may replace the chemical cross-links with cooperative H-bonds for creating a physically cross-linked dynamic PAMPS network dissipating energy under stress. However, previous works show that such physical hydrogels readily dissolve in water because of the AMPS counterions producing a high ionic osmotic pressure dominating over the elasticity of the physical network.[5,11,12]

We recently observed that UV polymerization of an aqueous solution of AMPS at its saturated concentration (60 wt %) in the absence of a chemical cross-linker leads to a PAMPS hydrogel absorbing 1000 times its weight in water without dissolving.[13] Because the hydrogel is easily soluble in chaotropic solvents such as the aqueous urea solutions, its network structure is solely formed by strong interchain H-bonds between AMPS units. It was also shown that, although 60 wt % is the saturated concentration of AMPS in water, another monomer, namely, *N*,*N*-dimethylacrylamide (DMAA), could be dissolved in this solution to increase the monomer content up to 80 wt %.[13] AMPS/DMAA copolymer hydrogels thus formed show a Young's modulus of 0.41 MPa, a tensile strength of 0.57 MPa, a high swelling degree in water, and self-healing behavior. Quantum mechanical calculations revealed that the good mechanical performance of the physical AMPS/DMAA hydrogels is due to the existence of strong interchain H-bonds between the copolymer chains.[13]

Our preliminary experiments showed that the replacement of DMAA with methacrylic acid (MAAc) as a comonomer of AMPS further improves the mechanical performance of the resulting copolymer hydrogels. The aim of this study was to

Received: December 3, 2022
Accepted: February 13, 2023
Published: February 22, 2023

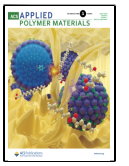

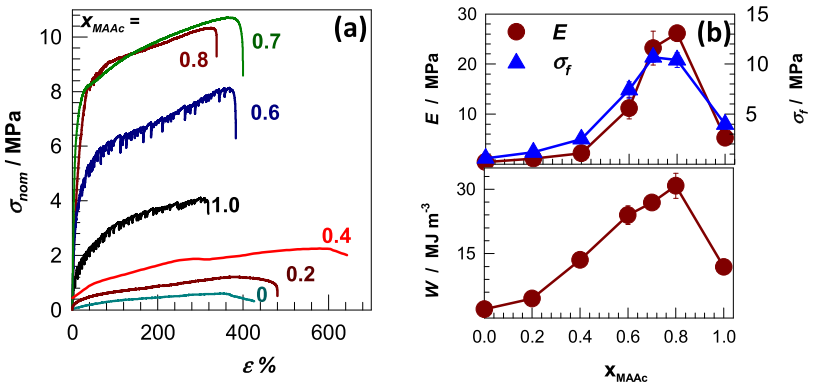

Figure 1. (a) Stress−strain curves of terpolymer hydrogels prepared at various x_{MAAc}. The amount of water at gel preparation (w) = 25 wt %. Strain rate $\dot{\varepsilon}$ = 1 min^{-1}. (b) Young's modulus E, fracture stress σ_f, and toughness W of the hydrogels plotted against x_{MAAc}.

investigate how the mechanical performance of superabsorbent AMPS/DMAA hydrogels varies by incorporating both DMAA and MAAc units into the gel network, which are H-bond donor and H-bond acceptor molecules, respectively. Hu et al. recently showed that the carboxylic group of MAAc and the carbonyl group of DMAA create multiple H-bonds between the copolymer chains, which are stabilized by the hydrophobic α-methyl groups of MAAc units.[14] However, these hydrogels exhibit a swelling ratio up to 78 in water due to the absence of a strong ionic comonomer such as AMPS. As will be seen below, the AMPS/MAAc/DMAA terpolymer hydrogels prepared at a MAAc/DMAA molar ratio of 4:1 exhibit 63-fold higher modulus compared to AMPS/DMAA hydrogels (26 MPa vs 0.41 MPa) without sacrificing their superabsorbent properties, i.e., they swell around 2000-fold in water without dissolving. We also show that increasing water content of the terpolymer hydrogels in their as-prepared state significantly affects their viscoelastic and mechanical properties due to the transition from uniform to colloidal gel structure composed of phase-separated and highly hydrogen-bonded AMPS-poor aggregates interconnected by AMPS-rich terpolymer chains.

2. RESULTS AND DISCUSSION

The hydrogels were synthesized by free-radical terpolymerization of AMPS, MAAc, and DMAA in an aqueous solution using Irgacure 2959 (0.2 mol % of the monomers) as the photoinitiator. All of the reactions were conducted at 23 ± 2 °C in a UV reactor at a wavelength of 360 nm. In our experiments, the molar fraction of MAAc + DMAA in the termonomer mixture was fixed at 0.62, with the rest being AMPS, to compare the data of the terpolymer hydrogels with those of AMPS/DMAA ones reported before.[13] Two sets of experiments were performed. In the first set, the amount of water (w) at gel preparation was fixed at 25 wt % as in our previous work,[13] while the MAAc content in the MAAc +DMAA mixture (x_{MAAc}) was varied. In the second set, x_{MAAc} was set to 0.80, while the water content w was changed between 25 and 95 wt % by diluting the gelation system with water.

2.1. Effect of x_{MAAc}. Figure 1a shows the nominal stress (σ_{nom})−strain (ε) curves of terpolymer hydrogels prepared at a fixed water content of 25 wt % and at various molar fractions of MAAc (x_{MAAc}). The curves denoted by 0 and 1.0 represent the data of AMPS/DMAA and AMPS/MAAc copolymer hydrogels, respectively. The terpolymer hydrogels with x_{MAAc} > 0.4 exhibit a much higher fracture stress σ_f compared to the copolymer hydrogels, and σ_f approaches a maximum value of around 10 MPa at x_{MAAc} = 0.70−0.80.

The mechanical parameters, namely, Young's modulus E, the fracture stress σ_f, and toughness W of the hydrogels, shown in Figure 1b reveal a significant improvement in all mechanical parameters when MAAc is included into the DMAA/AMPS network structure. Young's modulus E of the hydrogels increases with increasing MAAc content, and after attaining a maximum value of 26 ± 2 MPa at x_{MAAc} = 0.80, it again decreases. Thus, the maximum modulus is 63-fold higher than that of the AMPS/DMAA hydrogel, which is attributed to a significant strengthening of H-bonding interactions in AMPS/DMAA hydrogels after incorporation of MAAc units. Previous works also show that Young's modulus of MAAc/DMAA copolymer hydrogels reaches the maximum value at x_{MAAc} = 0.80.[14,15] Our recent theoretical calculations revealed that the hydrophobicity of MAAc units and the formation of strong H-bonded nanoaggregates during their copolymerization with DMAA are mainly responsible for the maximum strength of interchain H-bonds at a critical composition of x_{MAAc} = 0.80 deviating from 0.50.[15] One may speculate that this deviation from equimolar composition suggests the existence of consecutive H-bond donor and acceptor monomer units on adjacent copolymer chains, facilitating cooperative hydrogen bonding.[15] A similar trend is seen for the toughness W and fracture stress σ_f of the hydrogels exhibiting maximum values of 31 ± 5 MJ·m^{-3} and 11 ± 1 MPa at x_{MAAc} = 0.70 and 0.80, respectively (Table S1).

We observed that all hydrogels, when placed in an excess of water for a duration of 2 months, significantly swell but preserve their shape without dissolving. The gel fraction W_g, which is the weight fraction of the water-insoluble polymer, is presented in Figure 2a by the filled symbols plotted against x_{MAAc}. All of the terpolymer hydrogels including the copolymer hydrogels exhibit a W_g between 0.64 and 0.94 with a minimum at x_{MAAc} = 0.60. Figure 2b shows the equilibrium weight swelling ratio m_{rel} of the hydrogels with respect to the as-prepared state plotted against x_{MAAc}. Note that x_{MAAc} = 0 and 1 correspond to the AMPS/DMAA and AMPS/MAAc copolymer hydrogels, respectively. The terpolymer hydrogels exhibit a higher degree of swelling compared to the copolymer hydrogels, and m_{rel} reaches a maximum value of 2900 ± 130 at x_{MAAc} = 0.60. Moreover, m_{rel} of the hydrogels varies between 1070 and 2900, indicating their superabsorbency due to the strong polyelectrolyte AMPS units. For instance, Figure 2c shows the images of a hydrogel specimen prepared at x_{MAAc} =

https://doi.org/10.1021/acsapm.2c02085
ACS Appl. Polym. Mater. 2023, 5, 2043−2050

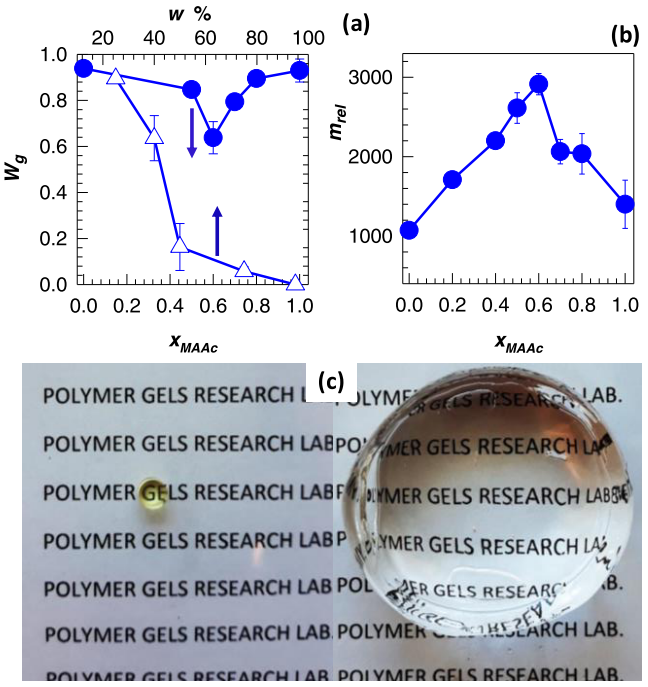

Figure 2. (a) Gel fraction W_g of terpolymer hydrogels plotted against x_{MAAc} at w = 25 wt % (circles) and against w% at x_{MAAc} = 0.80 (triangles). (b) Equilibrium weight swelling ratio m_{rel} of the hydrogels shown as a function of x_{MAAc}. (c) Images of a hydrogel specimen formed at w = 25 wt % and x_{MAAc} = 0.80 before (left) and after swelling in water (right).

0.80 before (left) and after (right) equilibrium swelling in water. The specimen absorbs 2035 ± 255 times its mass in water at equilibrium during which only 10% of the polymer dissolves (W_g = 0.9).

The question that may arise is as follows: what are the types of cross-links in the hydrogels making them stable in water? It could be argued that some chemical cross-links may form in the hydrogels because of the self-cross-link ability of DMAA units.[14,16] We conducted solubility tests on water-swollen hydrogels in aqueous solutions of urea, which is a well-known H-bond breaking agent. All of the hydrogels prepared at various x_{MAAc} and water contents could be dissolved in an aqueous 7 M urea solution within 2 weeks reflecting their physical nature. Because H-bonds are much weaker than the covalent bonds, this finding also suggests the existence of multiple H-bonds between the terpolymer chains strengthening the interchain interactions. We should note that the chain entanglements may also contribute to the strength of H-bonding interactions by restricting the mobility of the terpolymer chains.[17]

Owing to the physically cross-linked structure of the hydrogels, they exhibited time-dependent mechanical properties. Figure 3a presents stress−strain curves of the hydrogel with w = 30 wt % and x_{MAAc} = 0.80 obtained at various strain rates $\dot{\varepsilon}$ as indicated. In Figure 3b, the modulus E and fracture stress σ_f are shown as a function of the strain rate $\dot{\varepsilon}$. Both the stiffness E and the strength σ_f of the terpolymer hydrogels increase with increasing $\dot{\varepsilon}$, i.e., with decreasing experimental timescale, as expected for physical hydrogels. Moreover, the yield stress σ_y also increases with $\dot{\varepsilon}$ and shows a linear dependence when plotted against log ($\dot{\varepsilon}$) (Figure 3c). This is in agreement with the Eyring theory of the rate of breaking molecular bonds induced by mechanical stress[18−20]

$$\sigma_y = \frac{2kT}{V_a}(\ln \dot{\varepsilon}/\varepsilon_0) + \frac{2E_a}{V_a} \quad (1)$$

where E_a is the activation energy, ε_0 is the pre-exponential factor, V_a is the activation volume, and kT is the thermal energy. The solid line in Figure 3c is the best fit of eq 1 to the data yielding the activation volume V_a as 18 ± 1 nm^3/molecule. V_a can be considered as the volume of the polymer segments in the hydrogels involved in cooperative motion leading to yielding. Thus, the size of segments responsible for yielding is $V_a^{1/3}$ = 2.62 ± 0.05 nm, which is much larger than the monomer size. This reflects activation of several segments such as H-bonded domains in the hydrogels during yielding.

2.2. Effect of Water Content: Uniform-to-Colloidal Gel Transition. In this section, we fixed x_{MAAc} at 0.80, at which the Young's modulus reaches its maximum (Figure 1b), while the amount of water (w) at the gel preparation was varied over a wide range. Visual observation revealed the formation of transparent hydrogels at $w \leq 40$ wt %, while they became translucent at 50 wt % and finally opaque at 75 wt %. A further increase in w to ≥93 wt % resulted in a phase-separated system composed of a viscous solution and opaque gel (Figure 4a). Figure 5a,b shows the stress−strain curves and mechanical parameters of the terpolymer hydrogels formed at various water contents w. The inset to Figure 5a shows the same data in a semi-logarithmic plot. It is seen that the optically transparent-to-opaque transition in the hydrogels was accompanied with a dramatic decrease in their stiffness and mechanical strength. Both the modulus E and fracture stress

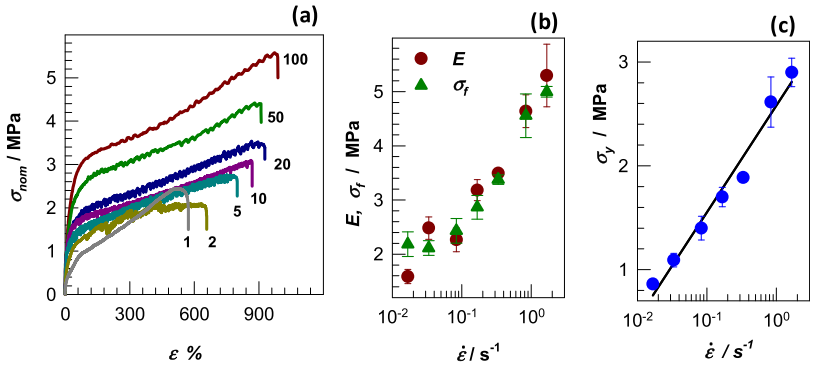

Figure 3. (a) Stress−strain curves of the hydrogel prepared at x_{MAAc} = 0.80 at various strain rates $\dot{\varepsilon}$ (in min^{-1}) as indicated; w = 30 wt %. (b) Strain rate dependences of the modulus E and fracture stress σ_f. (c) Yield stress σ_y plotted against log ($\dot{\varepsilon}$). The line is the best fit of eq 1 to the data.

https://doi.org/10.1021/acsapm.2c02085
ACS Appl. Polym. Mater. 2023, 5, 2043−2050

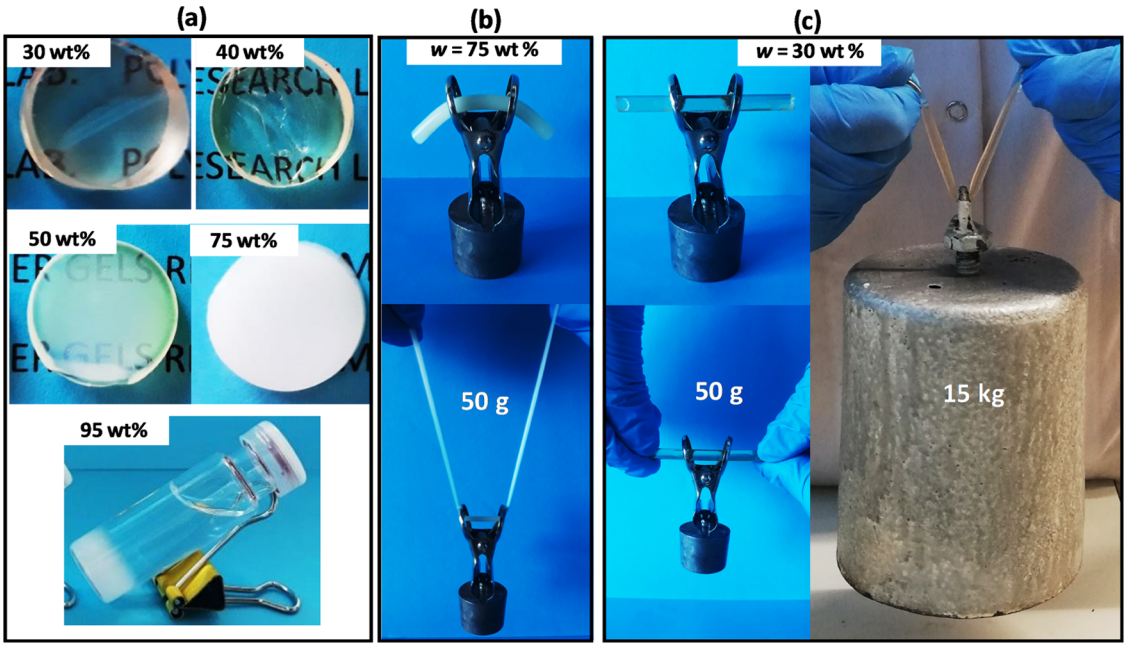

Figure 4. (a) Images of hydrogels formed at various w as indicated. (b, c) Images of hydrogel specimens formed at w = 75 wt % (b) and 30 wt % (c) under the gravity and under load indicated. The breaking load for the hydrogel with w = 30 wt % is 20 kg.

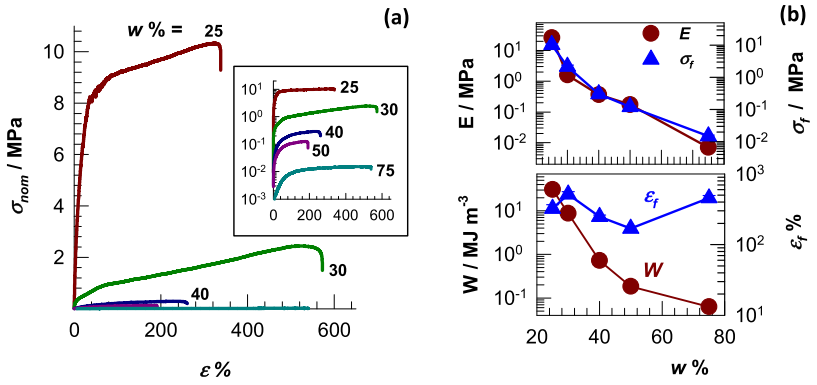

Figure 5. Stress−strain curves (a) and mechanical parameters (b) of terpolymer hydrogels formed at various water contents w; $\dot{\varepsilon}$ = 1 min^{-1}. ε_f is the fracture strain of the hydrogels.

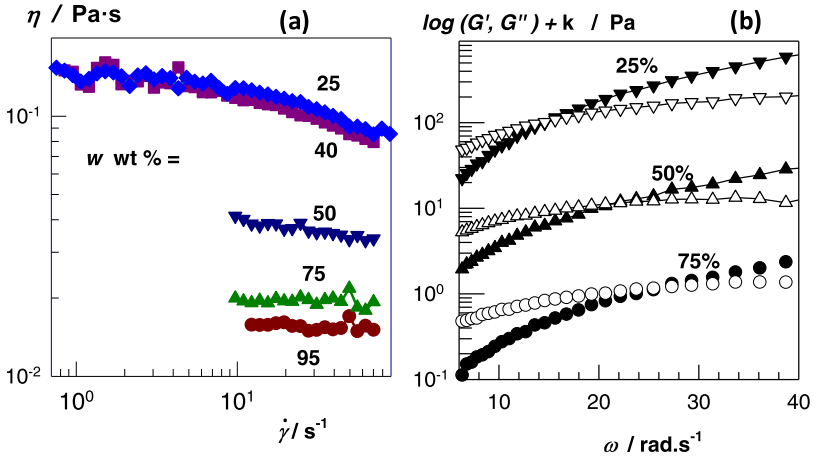

Figure 6. (a) Shear rate $\dot{\gamma}$ dependence of the viscosity η of aqueous terpolymer solutions isolated from hydrogels formed at various w indicated; polymer concentration = 1 w/v %; and temperature = 25 °C. (b) Storage modulus G' (filled symbols) and loss modulus G'' (open symbols) of the same terpolymer solutions shown as a function of the angular frequency ω. The vertical shift factor k = 0, 1, and 2 for w = 25, 50, and 75 wt %, respectively. γ_o = 0.1.

https://doi.org/10.1021/acsapm.2c02085
ACS Appl. Polym. Mater. 2023, 5, 2043−2050

σ_f decrease by 3 orders of magnitude (from 26 ± 2 MPa to 7 ± 1 kPa and 10.4 ± 0.7 MPa to 15 ± 1 kPa, respectively) with increasing w from 25 to 75 wt % (Table S2). Simultaneously, solubility tests revealed that the gel fraction W_g decreases from 90 ± 1 to 6 ± 2% with increasing w from 25 to 75 wt %, and finally they become soluble at w = 95 wt % (open symbols in Figure 2a). The drastic decrease in the stiffness and strength of the hydrogels is also illustrated in Figure 4b,c presenting the images of cylindrical hydrogel specimens formed at w = 75 wt % (b) and 30 wt % (c). The hydrogel formed at w = 75 wt % already deforms under the gravity and can be around 4 times stretched under a load of 50 g, while that formed at w = 30 wt % preserves its length under the same load and sustains 15 kg load.

For a deeper understanding of the origin of the optically transparent-to-opaque transition accompanied with a strong-to-weak transition with increasing water content, the primary terpolymer molecules constituting the hydrogel's network were isolated and characterized by viscosity and frequency sweep tests. For this purpose, the hydrogels formed at various w were solubilized in aqueous 7 M urea solutions, followed by dialyzing first against water and then aqueous PEG-10000 (4 wt %), each for 3 days. After isolation of the terpolymers by freeze-drying, they were dissolved in distilled water at a concentration of 1 w/v %. Note that, for the phase-separated hydrogel formed at w = 95 wt % (Figure 4a), the gel region was separated from the supernatant viscous solution and then solubilized. Figure 6a shows the viscosity η of aqueous terpolymer solutions at a fixed concentration of 1 w/v % plotted against the shear rate $\dot{\gamma}$. The lower the w, the higher the solution viscosity, indicating the formation of longer primary chains at a higher monomer concentration at gelation. Figure 6b shows the frequency (ω) sweep results of the same solutions isolated from hydrogels with w = 25, 50, and 75 wt %. The storage modulus G' and loss modulus G'' data were vertically shifted by a factor k to avoid overlapping. A typical behavior of a semidilute solution is seen in the figure, i.e., G'' exceeds G' at low frequencies, while there is a crossover between G' and G'' above which a transition from more liquid-like to more solid-like occurs. The crossover frequency ω_c decreases from 26 to 15 s^{-1} as w is decreased from 75 to 25 wt %, which is an indication of increasing number of interchain H-bonds between the primary chains. The results reveal that when compared to opaque hydrogels, transparent hydrogels formed at $w \leq 40$ wt % have longer polymer chains with a higher number of intermolecular H-bonds. The increasing number of H-bonds with increasing chain length can be explained with the proximity effect,[17,21,22] i.e., the preformed H-bond between two polymer chains restricts the mobility of the chain units in the vicinity of the first bond and hence facilitates the formation of subsequent H-bonds.

Moreover, the appearance of opacity and finally phase separation with increasing water content can be explained with the formation of strong H-bonded complexes between MAAc and DMAA units that cannot absorb all water in the hydrogel.[15] Because the water absorption capacity of highly H-bonded and hence highly physically cross-linked regions will be lower than that of the loosely cross-linked regions, a phase separation occurs at which a gel phase will separate out of the solution phase. This behavior was clearly observed for the hydrogel formed at w = 95 wt % (Figure 7a); the opaque phase-separated hydrogel in equilibrium with the viscous polymer solution does not flow under gravity and recovers its

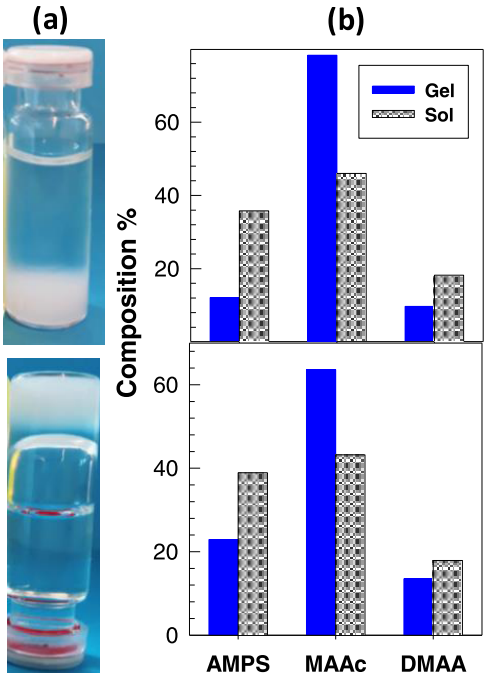

Figure 7. (a) Images of the phase-separated hydrogel before (up) and after turning the vial (down); w = 95 wt %. (b) Composition of the terpolymers in the sol and gel phases of the phase-separated hydrogels formed at w = 95 wt % (up) and 93 wt % (down).

shape and size after shaking. We should note that such a transparent-to-opaque transition with increasing water content was recently reported for PMAAc hydrogels prepared in the presence of TEMED capable of forming H-bond complexes.[23] Our recent molecular dynamic simulation results also predict aggregated configuration of the network chains in MAAc/DMAA hydrogels due to the formation of strong interchain H-bonds excluding water from the copolymer.[15]

To determine the composition of the terpolymer chains in both gel and sol phases, FTIR and elemental microanalysis measurements were conducted on dried hydrogel specimens taken from both phases. The analysis of the amide I region of the FTIR spectra reveals that the sol phase is rich in AMPS units, while MAAc units are enriched in the gel phase (Figures S1 and S2). To quantify the composition of the terpolymers in both phases, elemental analysis for C, N, and S was performed on phase-separated hydrogels formed at w = 93 and 95 wt %. Because S is the marker for AMPS ($C_7H_{13}NO_4S$), while N is the marker for both AMPS and DMAA (C_5H_9NO) but does not exist in MAAc ($C_4H_6O_2$), the distribution of the monomer units in the gel and sol phases was calculated and is shown in Figure 7b and Tables S3 and S4. For both hydrogels, the sol phase consists of around 37 mol % AMPS compared to 12−23 mol % in the gel phase (nominal value in the feed: 38 mol %), which seems to be responsible for the water solubility of the sol phase because of the dominating ionic osmotic pressure of AMPS counterions. Moreover, the gel phase is rich in MAAc units (64−78 mol % vs 43−46 mol % in the sol, nominal value: 49.6 mol %), resulting in a simultaneous increase in the MAAc mole fraction (x_{MAAc}) to 0.83−0.89, which is close to the critical x_{MAAc} to obtain mechanically strongest hydrogels (Figure 1b). Thus, the phase separation is due to the formation of a H-bonded complex between MAAc and DMAA units of the hydrogels, while polymer chains rich in

https://doi.org/10.1021/acsapm.2c02085
ACS Appl. Polym. Mater. 2023, 5, 2043−2050

AMPS units remain in the solution phase. Previous works on co- and terpolymerization of AMPS with AAm and/or acrylic acid (AAc) reveal that the reactivity ratio of AMPS is much smaller than that of AAm or AAc.[24,25] We may conclude that the AMPS-rich blocks formed after consumption of the more reactive DAAm and MAAc monomers locally absorb a large amount of water than the AMPS-poor, less swollen regions, resulting in a phase-separated hydrogel. Thus, the transparent hydrogel possessing a uniform network turns into a colloidal opaque hydrogel at w > 40 wt % at which it consists of less swollen, highly hydrogen-bonded, AMPS-poor phase-separated aggregates interconnected by loosely hydrogen-bonded AMPS-rich regions.

2.3. Large Strain Behavior. Large strain behavior of terpolymer hydrogels was studied using cyclic compression and tensile measurements. The hydrogel specimens were subjected to successive loading and unloading cycles with a time interval of 1 min between cycles up to a maximum strain ε_{max} below the fracture point. Figure 8a shows five successive compression cycles to ε_{max} = 80% for the hydrogel formed at w = 40 wt %, where the arrows indicate the loading (compression) and unloading steps. The unit of the strain in the figure is presented by the deformation ratio λ (= 1 − ε). It is seen that each unloading curve deviates from the previous loading, indicating breaking of some interchain bonds in the hydrogel. The lost (dissipated) energy U_{hys} due to this microscopic damage calculated as the area enveloped by the loading and unloading curves is a constant value, 191 ± 9 kJ·m^{-3}, i.e., the cycles are reversible independent of the number of cycles. The reversibility of the mechanical cycles reveals that the bonds broken after loading are repaired during the waiting time of 1 min between cycles. The reversibility remains unchanged when w is increased to 50 wt % at which a translucent hydrogel forms (Figure S3).

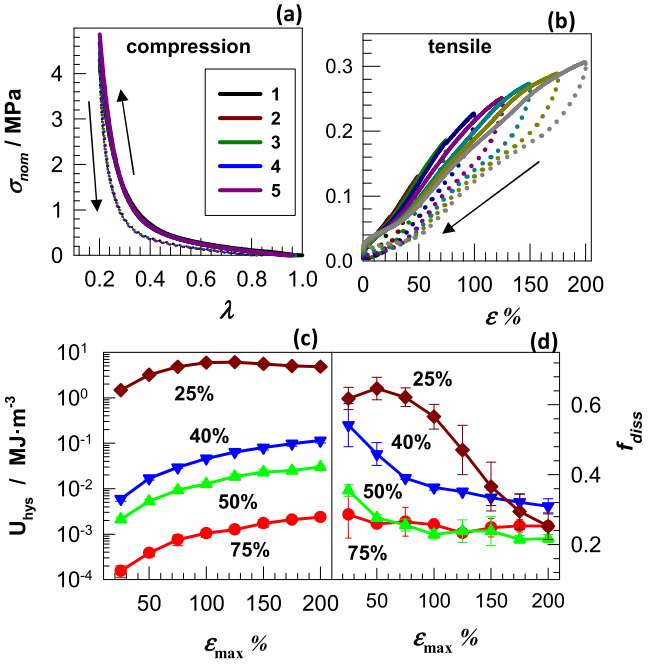

Figure 8. Cyclic compression and tensile tests conducted on hydrogel specimens with a time interval of 1 min between cycles; $\dot{\varepsilon}$ = 1 min^{-1}. (a) Five successive compressive cycles up to a maximum strain ε_{max} of 80% for the hydrogel formed at w = 40 wt %. (b) Eight successive tensile cycles for the same hydrogel. ε_{max} is increased from 25 to 200% with steps 25%. (c, d) U_{hys} and f_{diss} obtained from tensile cycles plotted against ε_{max}. w of the hydrogels is indicated.

Figure 8b shows eight successive tensile cycles for the hydrogel formed at w = 40 wt % with ε_{max} increasing from 25 to 200% in steps of 25%. Here again, each loading curve follows the previous loading as well as the stress−strain curve of the virgin sample (Figure S4). Similar results were also obtained using hydrogels formed between w = 25 and 75 wt %. (Figure S5). As seen in Figure 8c, U_{hys} increases with decreasing w or increasing ε_{max}, reflecting the increased extent of reparable damage in the hydrogels. To compare the dissipative properties of terpolymer hydrogels formed at various water contents, the fraction of the loading energy dissipated during each cycle (f_{diss}) is a better parameter as it gives the dissipated energy per loading energy and hence eliminates the differences in the mechanical performances of the hydrogels. For opaque hydrogels with w = 50 and 75 wt %, f_{diss} is around 25% and independent of ε_{max}, revealing that 25% of the loading energy is dissipated (Figure 8d). For transparent hydrogels with w = 25 and 40 wt %, f_{diss} is around 60% at low ε_{max}, while it decreases and approached the value of opaque hydrogels as ε_{max} is increased. The results thus show that less energy is dissipated from phase-separated hydrogels compared to the homogeneous ones. The reversibility of the mechanical cycles also indicates self-recoverability of the microstructure of the hydrogels after a microscopic damage. However, cut-and-heal tests revealed that the hydrogels do not have the ability to heal autonomously or under the effect of temperature, which is attributed to their high stiffness reducing the mobility of the chains.

3. CONCLUSIONS

PAMPS hydrogels are attractive materials due to their large water absorption capacity and find applications in water purification, bioengineering, agriculture, food engineering, and electrosensitive soft materials. Previous works show that the covalently cross-linked PAMPS hydrogels exhibit poor mechanical properties because of their covalently cross-linked network structure with low energy dissipation. Moreover, the physically cross-linked ones readily dissolve in water because of the AMPS counterions producing a high ionic osmotic pressure dominating over the elasticity of the physical network. Herein, we demonstrated that the terpolymerization of AMPS, MAAc, and DMAA in an aqueous solution under UV light without a chemical cross-linker produces mechanically strong hydrogen-bonded hydrogels that are stable in water. The hydrogel formed at a MAAc mole fraction x_{MAAc} = 0.8 exhibits a high Young's modulus (26 ± 2 MPa) and toughness (31 ± 5 MJ·m^{-3}) and is able to absorb 2035 ± 255 times its mass in water without dissolving. Although all hydrogels remain stable in water, they readily dissolve in aqueous urea solutions within 2 weeks, reflecting their hydrogen-bonded supramolecular structure. Because H-bonds are much weaker than covalent bonds, this finding also suggests the existence of multiple interchain H-bonds. An optically transparent-to-opaque transition accompanied with a mechanically strong-to-weak transition was observed with increasing water content of the hydrogels due to the transformation of the uniform network into a colloidal network composed of phase-separated and highly hydrogen-bonded AMPS-poor aggregates interconnected by AMPS-rich terpolymer chains.

https://doi.org/10.1021/acsapm.2c02085
ACS Appl. Polym. Mater. 2023, 5, 2043−2050

4. EXPERIMENTAL SECTION

4.1. Materials. 2-Acrylamido-2-methylpropane-1-sulfonic acid (AMPS, 99%, Sigma-Aldrich), methacrylic acid (MAAc, 99%, Merck), *N*,*N*-dimethylacrylamide (DMAA, 99%, Sigma-Aldrich), 2-hydroxy-4′-(2-hydroxyethoxy)-2-methylpropiophenone (Irgacure 2959, 98%, Sigma-Aldrich), and poly(ethylene glycol) (PEG, 10 000 g·mol^{-1}, Sigma-Aldrich) were used as received. Acrylic acid (AAc, 99%, Merck) was passed through an inhibitor removal column (Sigma-Aldrich) before use.

4.2. Hydrogel Preparation. The hydrogels were synthesized by terpolymerization of AMPS, MAAc, and DMAA using Irgacure 2959 (0.2 mol % of the monomers) as the photoinitiator. All of the reactions were conducted at 23 ± 2 °C in a UV reactor at a wavelength of 360 nm. In our experiments, the molar fraction of MAAc + DMAA in the termonomer mixture was fixed at 0.62 to compare the data of the terpolymer hydrogels with those of AMPS/DMAA ones reported before.[13] Two sets of experiments were conducted. In the first set, the water content w was fixed at 25 wt %, while the MAAc content in the comonomer mixture (x_{MAAc}) was varied. In the second set, x_{MAAc} was set to 0.80, while the amount of water was varied between 25 and 95 wt % by diluting the gelation system with water. The amounts of the monomers and water in the hydrogel preparation are collected in Tables S5 and S6. Typically, to prepare hydrogels at w = 25 wt % and x_{MAAc} = 0.80, AMPS (2.50 g, 12 mmol), MAAc (1.40 g, 16 mmol), and DMAA (0.40 g, 4.0 mmol) were dissolved in water (1.40 g). After bubbling nitrogen through the homogeneous solution for 10 min, the Irgacure photoinitiator (15 mg, 0.2 mol % of the monomers) was added. The solution was then transferred to 1 mL plastic syringes, and the polymerization reactions were performed in an UV reactor at 360 nm for 24 h.

4.3. Characterization. For the swelling tests in water, the as-prepared hydrogels were taken out of the syringes and cut into cylindrical specimens with a diameter of 4.6 mm and a length of around 3 mm. They were then immersed in excess distilled water at 23 ± 2 °C during which water was refreshed every 2nd day. The swelling equilibrium of the samples was checked by weighing the specimens. All samples reached their equilibrium state in water within 2 weeks. After reaching swelling equilibrium, the specimens were taken out of the deionized water and freeze-dried (Christ Alpha 2e4 LD-plus). The equilibrium swelling ratio m_{rel} with respect to the preparation state was calculated as m/m_0, where m and m_0 are the masses of the specimen after equilibrium swelling and after preparation, respectively. The gel fraction W_g, i.e., the conversion of monomers to the water-insoluble polymer (mass of water-insoluble polymer / initial mass of the monomer), was calculated from the masses of dry, extracted polymer network and from the comonomer feed.

The solubilization of the hydrogels was carried out by immersing as-prepared hydrogel specimens in an excess of aqueous 7 M urea solution under stirring for 2 weeks at 23 ± 2 °C. All of the terpolymer hydrogels could be dissolved in this solution. The homogeneous polymer solutions thus obtained were then poured into dialysis tubing (3500 MWCO, SnakeSkin, Pierce) and dialyzed for 3 days against water and additional 3 days against 4 wt % PEG-10000 to concentrate the solution. The concentrated solution was then freeze-dried on a Christ Alpha 2-4 LD-plus freeze-dryer. For the viscosity measurements, 20 mg of the terpolymers isolated from the hydrogels was dissolved in 2 mL of distilled water.

FTIR spectra of dried hydrogels were collected using an Agilent spectrometer (Carry 630, Agilent Technology) with ATR assembly. Elemental analyses were performed on a CHNS-932 (LECO) elemental analyzer. Rheological measurements were conducted at 25 °C on a temperature-controlled Gemini 150 rheometer system (Bohlin Instruments). The viscosities η of the terpolymer solutions were measured using a cone-and-plate geometry (cone angle: 4°, diameter: 40 mm) between shear rates of 1×10^{-3} and 1×10^{2} s^{-1}. The frequency dependence of the dynamic moduli of the same solutions was measured at a strain amplitude γ_0 of 0.1. The mechanical performances of terpolymer hydrogels were determined at 23 ± 2 °C on a Zwick Roell Z0.5 TH testing machine using a 500 N load cell. The cylindrical hydrogel samples (diameter: 4.6 mm, length: 60 mm) were subjected to uniaxial stretching and compression tests. The stress was presented by its nominal value σ_{nom}, which is the force per cross-sectional area of the undeformed gel specimen, while the strain ε is defined as the change in the sample length relative to the initial length of the gel specimen. The modulus E was calculated from the linear region of the stress−strain curves (between 5 and 15% strain), while the toughness W was calculated by integrating the area underneath the stress−strain curve up to the fracture point.

■ ASSOCIATED CONTENT

Supporting Information

The Supporting Information is available free of charge at https://pubs.acs.org/doi/10.1021/acsapm.2c02085.

Details of the synthesis and properties of the hydrogels, FTIR characterization, and cyclic mechanical test results (PDF)

■ AUTHOR INFORMATION

Corresponding Authors

Esra Su − *Faculty of Aquatic Sciences, Istanbul University, 34134 Fatih, Istanbul, Turkey*; Phone: +90 539 301 2726; Email: esra.su@istanbul.edu.tr

Oguz Okay − *Department of Chemistry, Istanbul Technical University, 34469 Maslak, Istanbul, Turkey*; orcid.org/0000-0003-2717-4150; Phone: +90 212 285 3156; Email: okayo@itu.edu.tr

Author

Busra Sekizkardes − *Department of Chemistry, Istanbul Technical University, 34469 Maslak, Istanbul, Turkey*; Present Address: Department of Material Science and Technology, Turkish-German University, 34820 Beykoz, Istanbul, Turkey; orcid.org/0000-0002-7460-9834

Complete contact information is available at: https://pubs.acs.org/10.1021/acsapm.2c02085

Author Contributions

The manuscript was written through contributions of all authors. All authors have given approval to the final version of the manuscript.

Funding

The authors thank METU Central Laboratory for elemental analysis. B.S. thanks to the TÜBİTAK BIDEB National Scholarship Program. O.O. thanks the Turkish Academy of Sciences (TUBA) for the partial support.

Notes

The authors declare no competing financial interest.

■ REFERENCES

(1) Fisher, L. W.; Sochor, A. R.; Tan, J. S. Chain Characteristics of Poly(2-acrylamido-2-methylpropanesulfonate) Polymers. 1. Light-Scattering and Intrinsic-Viscosity Studies. *Macromolecules* **1977**, *10*, 949−954.

(2) Tong, Z.; Liu, X. Swelling Equilibria and Volume Phase Transition in Hydrogels with Strongly Dissociating Electrolytes. *Macromolecules* **1994**, *27*, 844−848.

(3) Liu, X.; Tong, Z.; Hu, O. Swelling Equilibria of Hydrogels with Sulfonate Groups in Water and in Aqueous Salt Solutions. *Macromolecules* **1995**, *28*, 3813−3817.

(4) Durmaz, S.; Okay, O. Acrylamide/2-Acrylamido-2-Methyl Propane Sulfonic Acid Sodium Salt-Based Hydrogels: Synthesis and Characterization. *Polymer* **2000**, *41*, 3693−3704.

(5) Su, E.; Okay, O. Hybrid Cross-Linked Poly(2-Acrylamido-2-Methyl-1-Propanesulfonic acid) Hydrogels with Tunable Viscoelastic, Mechanical and Self-Healing properties. *React. Funct. Polym.* **2018**, *123*, 70−79.
(6) Boonkaew, B.; Barber, P. M.; Rengpipat, S.; Supaphol, P.; Kempf, M.; He, J.; John, V. T.; Cuttle, L. Production with Gamma Irradiation Creates Silver Nanoparticles and Radical Polymerization. *J. Pharm. Sci.* **2014**, *103*, 3244−3253.
(7) Yang, C.; Liu, Z.; Chen, C.; Shi, K.; Zhang, L.; Ju, X.-J.; Wang, W.; Xie, R.; Chu, L. Y. Reduced Graphene Oxide-Containing Smart Hydrogels with Excellent Electro-Response and Mechanical Properties for Soft Actuators. *ACS Appl. Mater. Interfaces* **2017**, *9*, 15758−15767.
(8) Jones, A.; Vaughan, D. Hydrogel Dressings in the Management of a Variety of Wound Types: A Review. *J. Orthop. Nurs.* **2005**, *9*, S1−S11.
(9) Gong, J. P.; Kurokawa, T.; Narita, T.; Kagata, G.; Osada, Y.; Nishimura, G.; Kinjo, M. Synthesis of Hydrogels with Extremely Low Surface Friction. *J. Am. Chem. Soc.* **2001**, *123*, 5582−5583.
(10) Nalampang, K.; Panjakha, R.; Molloy, R.; Tighe, B. J. Structural Effects in Photopolymerized Sodium AMPS Hydrogels Crosslinked with Poly(ethylene glycol) Diacrylate for Use as Burn Dressings. *J. Biomater. Sci., Polym. Ed.* **2013**, *24*, 1291−1304.
(11) Xing, X.; Li, L.; Wang, T.; Ding, Y.; Liu, G.; Zhang, G. A Self-Healing Polymeric Material: From Gel to Plastic. *J. Mater. Chem. A* **2014**, *2*, 11049−11053.
(12) Kazantsev, O. A.; Igolkin, A. V.; Shirshin, K. V.; Kuznetsova, N. A.; Spirina, A. N.; Malyshev, A. P. Spontaneous Polymerization of 2-Acrylamido-2-Methylpropanesulfonic Acid in Acidic Aqueous Solutions. *Russ. J. Appl. Chem.* **2002**, *75*, 465−469.
(13) Su, E.; Yurtsever, M.; Okay, O. A Self-Healing and Highly Stretchable Polyelectrolyte Hydrogel via Cooperative Hydrogen Bonding as a Superabsorbent Polymer. *Macromolecules* **2019**, *52*, 3257−3326.
(14) Hu, X.; Vatankhah-Varnoosfaderani, M.; Zhou, J.; Li, Q.; Sheiko, S. S. Weak Hydrogen Bonding Enables Hard, Strong, Tough, and Elastic Hydrogels. *Adv. Mater.* **2015**, *27*, 6899−6905.
(15) Erkoc, C.; Yildirim, E.; Yurtsever, M.; Okay, O. Roadmap to Design Mechanically Robust Copolymer Hydrogels Naturally Cross-Linked by Hydrogen Bonds. *Macromolecules* **2022**, *55*, 10576−10589.
(16) Cipriano, B. H.; Banik, S. J.; Sharma, R.; Rumore, D.; Hwang, W.; Briber, R. M.; Raghavan, S. R. Superabsorbent Hydrogels That Are Robust and Highly Stretchable. *Macromolecules* **2014**, *47*, 4445−4452.
(17) Song, G.; Zhang, L.; He, C.; Fang, D.-C.; Whitten, P. G.; Wang, H. Facile Fabrication of Tough Hydrogels Physically Cross-Linked by Strong Cooperative Hydrogen Bonding. *Macromolecules* **2013**, *46*, 7423−7435.
(18) Kauzmann, W.; Eyring, H. The Viscous Flow of Large Molecules. *J. Am. Chem. Soc.* **1940**, *62*, 3113−3125.
(19) Sweeney, J.; Ward, I. M. *Mechanical Properties of Solid Polymers*; John Wiley & Sons, 2012.
(20) McCrum, N. G.; Buckley, C. P.; Buckley, C.; Bucknall, C. *Principles of Polymer Engineering*; Oxford University Press: USA, 1997; pp 184−197.
(21) Kříž, J.; Dybal, J.; Brus, J. Cooperative Hydrogen Bonds of Macromolecules. 2. Two-Dimensional Cooperativity in the Binding of Poly(4-vinylpyridine) to Poly(4-vinylphenol). *J. Phys. Chem. B* **2006**, *110*, 18338−18346.
(22) Kříž, J.; Dybal, J. Cooperative Hydrogen Bonds of Macromolecules. 3. A Model Study of the Proximity Effect. *J. Phys. Chem. B* **2007**, *111*, 6118−6126.
(23) Zhang, X. N.; Du, C.; Wei, Z.; Du, M.; Zheng, Q.; Wu, Z. L. Stretchable Sponge-like Hydrogels with a Unique Colloidal Network Produced by Polymerization-Induced Microphase Separation. *Macromolecules* **2022**, *55*, 1424−1434.
(24) Scott, A. J.; Riahinezhad, M.; Penlidis, A. Optimal Design for Reactivity Ratio Estimation: A Comparison of Techniques for AMPS/Acrylamide and AMPS/Acrylic Acid Copolymerizations. *Processes* **2015**, *3*, 749−768.
(25) Scott, A. J.; Kazemi, N.; Penlidis, A. AMPS/AAm/AAc Terpolymerization: Experimental Verification of the EVM Framework for Ternary Reactivity Ratio Estimation. *Processes* **2017**, *5*, No. 9.

https://doi.org/10.1021/acsapm.2c02085
ACS Appl. Polym. Mater. 2023, 5, 2043−2050